# DISCOVERY OF MULTIPLE PULSATIONS IN THE NEW $\delta$ SCUTI STAR HD 92277: ASTEROSEISMOLOGY FROM DOME A, ANTARCTICA

WEIKAI ZONG[1,2,3], JIAN-NING FU[1,4], JIA-SHU NIU[1], S. CHARPINET[2,3], G. VAUCLAIR[2,3], MICHAEL C. B. ASHLEY[5], XIANGQUN CUI[6], LONGLONG FENG[7], XUEFEI GONG[6], JON S. LAWRENCE[5,8], DANIEL LUONG-VAN[5], QIANG LIU[9], CARL R. PENNYPACKER[10], LINGZHI WANG[9], LIFAN WANG[7,11], XIANGYAN YUAN[7,12], DONALD G. YORK[13], XU ZHOU[9], ZHENXI ZHU[7], AND ZONGHONG ZHU[1]

[1] Department of Astronomy, Beijing Normal University, Beijing 100875, China
[2] Université de Toulouse, UPS-OMP, IRAP, F-31400 Toulouse, France; jnfu@bnu.edu.cn
[3] CNRS, IRAP, 14 Av. E. Belin, F-31400 Toulouse, France
[4] Visiting Astronomer at Xinjiang Astronomical Observatory, Chinese Academy of Sciences, Urumqi 830011, China
[5] School of Physics, University of New South Wales, Sydney, NSW 2052, Australia
[6] Nanjing Institute of Astronomical Optics and Technology, Nanjing 210042, China
[7] Purple Mountain Observatory, Chinese Academy of Sciences, Nanjing 210008, China
[8] Australian Astronomical Observatory, Epping, NSW 1710, Australia
[9] National Astronomical Observatories, Chinese Academy of Sciences, Beijing 100012, China
[10] Center for Astrophysics, Lawrence Berkeley National Laboratory, Berkeley, CA, USA
[11] Department of Physics & Astronomy, Texas A&M University, College Station, TX 77843, USA
[12] Chinese Center for Antarctic Astronomy, Nanjing 210008, China
[13] Department of Astronomy and Astrophysics and Enrico Fermi Institute, University of Chicago, Chicago, IL 60637, USA

## ABSTRACT

We report the discovery of low-amplitude oscillations in the star HD 92277 from long, continuous observations in the $r$ and $g$ bands using the CSTAR telescopes in Antarctica. A total of more than 1950 hours of high-quality light curves were used to categorize HD 92277 as a new member of the $\delta$ Scuti class. We have detected 21 (20 frequencies are independent and one is the linear combination) and 14 (13 frequencies are independent and one is the linear combination) pulsation frequencies in the $r$ and $g$ bands, respectively, indicating a multi-periodic pulsation behavior. The primary frequency $f_1 = 10.810\,\mathrm{days}^{-1}$ corresponds to a period of 0.0925 days and is an $l = 1$ mode. We estimate a $B - V$ index of 0.39 and derive an effective temperature of 6800 K for HD 92277. We conclude that long, continuous and uninterrupted time-series photometry can be performed from Dome A, Antarctica, and that this is especially valuable for asteroseismology where multi-color observations (often not available from space-based telescopes) assist with mode identification.

*Key words:* stars: individual (HD 92277) – stars: variables: delta Scuti – techniques: photometric

*Supporting material:* data behind figures

## 1. INTRODUCTION

Asteroseismology is a powerful method to probe the interior of pulsating stars. Different oscillation modes penetrate to different depths inside the pulsating stars, providing important information about their otherwise unobservable interiors. To detect as many oscillation modes as possible, astronomers have employed telescope networks in temperate sites around the Earth to obtain long periods of continuous photometric data without diurnal aliasing. Examples of such networks include the "Whole Earth Telescope" (Nather et al. 1990), the "STEllar PHotometry International" (Michel et al. 1992), and the "Global Oscillation Network Group" (Harvey et al. 1996). In this new century, two possibilities have emerged for uninterrupted time-series photometry. The first one is using space telescopes such as *Microvariability and Oscillations of Stars* (Matthews 2007), *CoRoT* (e.g., Baglin et al. 2006), and *Kepler* (Borucki et al. 2010). While the main aim of the *Kepler* mission was to search for exoplanets using the transit method, the resultant high-precision photometric data are suitable for studying variable stars, including pulsating stars, using asteroseismology. The second possibility is conducting observations from polar sites where there is continuous darkness for months and many stars are circumpolar. Examples of studies where polar sites have advantages include searching for exoplanets (e.g., Deeg et al. 2005; Pont & Bouchy 2005),

stellar rotation and activity (e.g., Strassmeier & Oláh 2004), and asteroseismology (e.g., Fossat 2005; Mosser & Aristidi 2007). The excellent atmospheric conditions above the Antarctic plateau have triggered the enthusiasm of astronomers and astrophysicists worldwide in recent decades (Ashley 2013 and references therein). For asteroseismology, the main advantages of Antarctica are the high fraction of clear weather, the low noise from atmospheric scintillation, the long periods of darkness, no diurnal aliasing, and low air mass variations as a result of the extreme southern latitude.

In 2008, China established Kunlun Station, its first astronomical site in Antarctica, at Dome A at longitude 77° 06′57″ E, latitude 80°25′08″ S. It is the highest point on the high Antarctic plateau with an elevation of 4013 m. Dome A is expected to have astronomical conditions similar to or better than those at Concordia Station at Dome C, based on their topographic similarities and comparison of altitudes (Saunders et al. 2009). Dome C has a median seeing of 0.23 arcsec at 500 nm—and correspondingly low scintillation noise—when observations are made from above the turbulent boundary layer 33 m above the ice (Lawrence et al. 2004). The median boundary layer height at Dome A is 14 m (Bonner et al. 2010), making the free atmosphere more easily accessible than it is at Dome C. Dome Fuji is another potentially excellent site on the Antarctic plateau (Okita et al. 2013).

The first-generation optical telescopes at Dome A were those of the Chinese Small Telescope ARray (CSTAR; Liu & Yuan 2009) and were deployed in 2008 January, supported by the PLATO observatory (Lawrence et al. 2009; Yang et al. 2009). CSTAR consisted of four co-mounted 14.5 cm telescopes pointed without tracking at the south celestial pole. One telescope was unfiltered, the other three had fixed Sloan $g$, $r$, and $i$ filters. CSTAR collected data autonomously for four winters, with no humans on site. Various issues resulted in CSTAR's $i$-band telescope being the only one working at peak performance and able to collect a mass of scientific data. With the first year's data, Zou et al. (2010) investigated the statistics of sky brightness and transparency, and Zhou et al. (2010a) published a catalog of about 10,000 stars. Using the $i$-band data from 2008 and 2010, Wang et al. (2011, 2013) reported observations of 222 variable stars, about four times the number of variables known from previous surveys of this region. In 2012 January, CSTAR was replaced by the first of three second-generation Chinese Antarctic Survey Telescopes (AST3; Yuan et al. 2010) at Kunlun Station, Dome A.

$\delta$ Scuti stars are variable stars of spectral type A or F with pulsation periods between 0.02 and 0.25 days. They are situated either in the classical Cepheid instability strip on the main sequence or are moving toward the giant branch on the H-R diagram (Breger 2000). Long and continuous photometric time-series observations improve the frequency resolution, enabling one to detect more closely spaced pulsations. For example, Strassmeier et al. (2008) investigated the low-amplitude $\delta$ Scuti star V1034 Centauri using data collected over 10.15 days in 2007 July with a duty cycle of 98% using the 25 cm sIRAIT telescope at Dome C. They confirmed the known fundamental period of 0.2 days and detected 23 new periods with a photometric precision of 3 and 4 mmag in $V$ and $R$, respectively, over a period of 2.4 hr.

The CSTAR telescopes observed thousands of stars simultaneously in an excellent stable atmosphere and with long time coverage. The photometric precision for bright stars reached the few mmag range (Wang et al. 2011, 2013), similar to the results from Dome C. One of the bright stars in CSTAR's field of view (FOV; see Section 2), HD 92277 = HIP 49368 = CSTAR 55150 ($\alpha = 10^{\rm h}04^{\rm m}40\overset{\rm s}{.}365$, $\delta = -88°40'$ $25\overset{''}{.}56$, 2000.0, $B - V = 0.375$, van Leeuwen 2007; $B = 9\overset{\rm m}{.}49$ and $V = 9\overset{\rm m}{.}10$, Høg et al. 2000), has a proper motion of $-21.64 \pm 0.84$ mas yr$^-$ in R.A., $14.22 \pm 0.82$ mas yr$^-$ in decl. and a parallax of $2.12 \pm 0.91$ mas (van Leeuwen 2007). It is known to be a multiple-star system in the Constellation Octans (Fabricius & Makarov 2000) and a white subgiant star with a spectral type of F0IV/V (Houck & Cowley 1975). Up until now, it has not been classified as a variable star. Using CSTAR data from 2009, we categorize this star as a $\delta$ Scuti variable and have used it to test the potential of asteroseismology at Dome A.

We present the analysis of data collected with two CSTAR telescopes, those with $g$ and $r$ filters, obtained in the winter of 2009 from April to July for the newly discovered $\delta$ Scuti star HD 92277. We describe the 2009 observations from CSTAR in Section 2 and the data reduction process in Section 3. Section 4 reports the pulsation analysis, while Section 5 presents the discussion. In the last section, we give our summary, conclusions, and prospects for future work. It is shown that time-series photometry can be conducted very well from Dome

**Table 1**
Log of Observations of CSTAR in 2009

| Month | No. of Images $g$ band | Exposure Time (hr) | No. of Images $r$ band | Exposure Time (hr) |
|-------|------------------------|--------------------|------------------------|--------------------|
| Mar | 35843 | 50.7 | 94877 | 203.7 |
| Apr | 105026 | 304.5 | 115408 | 334.6 |
| May | 106802 | 593.3 | 106646 | 592.5 |
| Jun | 3639 | 20.2 | 112446 | 624.7 |
| Jul | ⋯ | ⋯ | 106480 | 591.6 |
| Total | 251310 | 968.7 | 536383 | 2348.6 |

A, Antarctica, which has some potential for the field of asteroseismology.

## 2. OBSERVATIONS

CSTAR operated for four consecutive winters from 2008 January. CSTAR is composed of four identical 14.5 cm telescopes, each of which has a FOV of $4.5 \times 4.5$ deg$^2$ on a common mount, all pointed at a fixed position very near to the south celestial pole. Each telescope is equipped with an ANDOR DV435 $1K \times 1K$ frame-transfer CCD, with 13 $\mu$m pixels, operating at ambient temperature. The frame-transfer CCD was chosen since it allowed shutterless operation, which was a priority for the prototype instrument to avoid mechanical failures, but also meant that bias and dark frames could not be taken. Three different fixed filters (Sloan $g$, $r$, and $i$) were mounted on three of the telescopes, while the fourth telescope had no filter. Due to the deliberate lack of a tracking mount, the stars traced circles on the CCD frames over a sidereal day, but only moved a small fraction of a pixel during an exposure time, typically 20 s. There are no moving parts used in normal telescope operations, and there is no human attendant during the observing season. The CSTAR telescopes worked at weather conditions of sky brightness below 10,000 ADU/pixel. A more detailed description of CSTAR can be found in Zhou et al. (2010a) and Liu & Yuan (2009).

The two CSTAR telescopes equipped with the $r$ and $g$ filters collected a large amount of valuable data. The observations in the $r$ band began on February 2 and ended on 2009 July 30, while the observations in the $g$ band covered 2009 March 7 to June 1. In the $r$ band, we obtained 536,383 images for a total exposure time of 2348 hr, with exposure times from 5 to 30 s. In the $g$ band, we collected 231,310 images for a total exposure time of 968.7 hr, using the same exposure times. The number of images obtained and the total exposure time per month are listed in Table 1. Table 2 gives the details of the exposure time used during the observations in both bands for the 2009 Antarctic winter. The duty cycle of our observations of HD 92277 in 2009 were 54% and 70% in the $r$ and $g$ bands, respectively. The duty cycle defined here is the total integral exposure time of scientific data over the whole exposure time in the Antarctic winter. The sky brightness in the two bands was investigated by Zong et al. (2014), and the effect of airglow and aurorae on observations at Dome A by Sims et al. (2012). The sky brightness (normal or auroral) was never high enough or rapidly changing enough to adversely affect the measurements of variability for the scientific data due to the differential measurement technique described in the next section.

**Table 2**
Exposure Time and Number of Images During the Observations in 2009

| Exp. (s) | Start | $g$-band End | No. of Images | Start | $r$-band End | No. of Images |
|---|---|---|---|---|---|---|
| 30 | Mar 7 | Mar 12 | 8 | … | … | … |
| 10 | Mar 12 | Mar 20 | 620 | Feb 2 | Mar 20 | 53060 |
| 5 | Mar 20 | Apr 14 | 102170 | Mar 20 | Apr 14 | 115922 |
| 20 | Apr 14 | Jun 1 | 148512 | Apr 14 | Jul 30 | 367401 |

**Table 3**
Basic Properties of the Comparison Star and Check Stars

| Object | R.A. (2000.0) | Decl. (2000.0) | $B$ (mag) | $V$ (mag) |
|---|---|---|---|---|
| C=HD 93426 | $10^h15^m20^s.205$ | $-88°42'00.96''$ | 10.97(6) | 9.62(2) |
| CH1=HD 98784 | $08^h58^m34^s.424$ | $-89°49'52.42''$ | 9.85(3) | 8.75(1) |
| CH2=HD 99685 | $09^h56^m37^s.829$ | $-89°46'56.74''$ | 7.93(-) | 7.84(-) |

## 3. DATA REDUCTION

### 3.1. Preliminary Data Reduction and Photometry

Bias subtraction and flat-field correction were applied to the raw CCD images without dark subtraction, which was negligible. The CCD was operated, without cooling Dewars, at the ambient Dome A temperature around −80 °C over the whole Antarctic winter. Two bias frames were acquired during the instrument test at Xinglong Station in China prior to deployment to Antarctica. We combined two super-flats, one in each band, by taking median frames of carefully selected samples of 320 and 267 images with relatively high sky brightnesses, 7000–7600 ADU in the $g$ band and 5000–5800 ADU in the $r$ band, obtained from March 20 to 22 and from 2009 March 15 to 22, respectively.

We used the images with 20 s exposure time for aperture photometry. In good weather conditions, more than 6000 stars up to 14.5 mag and about 5000 stars up to 14 mag were detected on each frame in $r$ and $g$, respectively. The telescopes were not perfectly focused, which limited the number of stars, but probably improved our photometric accuracy due to less influence from intrapixel sensitivity variations. The $r$ frames with exposure times of 20 s were discarded when the number of stars on these images totaled less than 2000 when the sky brightness was very low, as shown in both the $g$- and $r$-band telescopes. Those discarded images were collected from 2009 April 14 to 23. We presume that a technical problem (perhaps icing on the telescope optics) had affected the $r$-band telescope during this period.

Table 3 lists the basic information of the comparison star HD 93426 and the two check stars HD 98784 and HD 99685. After the initial reduction, the resulting 326,115, and 148,512 images in the $r$ band and the $g$ band underwent aperture photometry using the DAOPHOT routine within IRAF.[14] About 99,000 abnormal data points in the $r$ band and 35,000 in the $g$ band were discarded since these points were affected by either large atmospheric extinction, high sky level, or contamination from satellite trails on the images. There were still a few data points that differed significantly from the local standard deviation in the light curves. We discarded these data points by applying a

five-pass $3\sigma$ clipping filter using a third-order polynomial fit to 100 nearby data points.

### 3.2. Photometric and Time Calibration

#### 3.2.1. Photometric Calibration

We used the catalog of calibrated $g$, $r$, $i$, and $z$ magnitudes of Tycho stars (Ofek 2008) for our photometric calibration, the same method used by Wang et al. (2011). The selected stars in the range $7 < [g, r] < 12$ mag and $\delta < -88°$ in Vizier[15] were matched to objects on the frames in good weather conditions recorded in the first quarter of 2009 May 17. Our photometry used an aperture of five pixels in the radius. We derived zeropoints of $3.93 \pm 0.10$ mag and $3.76 \pm 0.10$ mag in $r$ and $g$ based on 63 and 51 stars, as shown in Figures 1(a) and (b), respectively.

#### 3.2.2. Time Calibration

The failure of a GPS time source meant that the raw times recorded with the images were based on uncorrected computer times. We derived the drift rates of the computer clocks by using the methods described in Zhou et al. (2010b). Figure 2 shows the difference between the two computer times of the telescopes and UTC calculated using star positions on the CCD frames. The computer time of the $g$-band telescope ran fast by 1.03 s per day for its entire run. For the $r$-band telescope, the clock ran slowly by 1.03 s per day and there was a time jump of 40 s on 2009 June 9. The start offset times (2009 March 30) were derived by using the times of minimum light of two eclipsing binary stars, CSTAR 57775 and CSTAR 38663, between 2008 and 2009. We assumed there were no period changes for those two eclipsing binary stars in these two years and derived the start offset time of 0.2095(6) days and 0.2071(6) days in the $g$ and $r$ bands, respectively.

### 3.3. Time-series Photometry

#### 3.3.1. Photometric Precision

We conducted photometry in a series of apertures (radii of 2.5, 3.0, …, 5.5 pixels). The optimized aperture for the stars depended on their minimum photometric scatters in magnitude. Figure 3 shows photometric scatters for the bright stars (<10 mag) with the optimized aperture over a period of 6 hr of the first quarter on 2009 May 17. As can be seen from Figure 3, the system can be used to determine relative magnitudes with a precision of several millimag on these short timescales. This enables one to study pulsators with amplitudes from ∼0.01 to 0.1 mag, e.g., $\delta$ Scuti stars, $\beta$ Cephei (Stankov & Handler 2005), and $\gamma$ Doradus (Kaye et al. 1999) variables. For stars with magnitudes in the range $10 < [r, g] < 13$, the photometric precision is 0.1 mag or better, which is suitable for

---

[14] IRAF is distributed by the National Optical Astronomy Observatory, which is operated by the Association of Universities for Research in Astronomy, Inc., under cooperative agreement with the National Science Foundation.
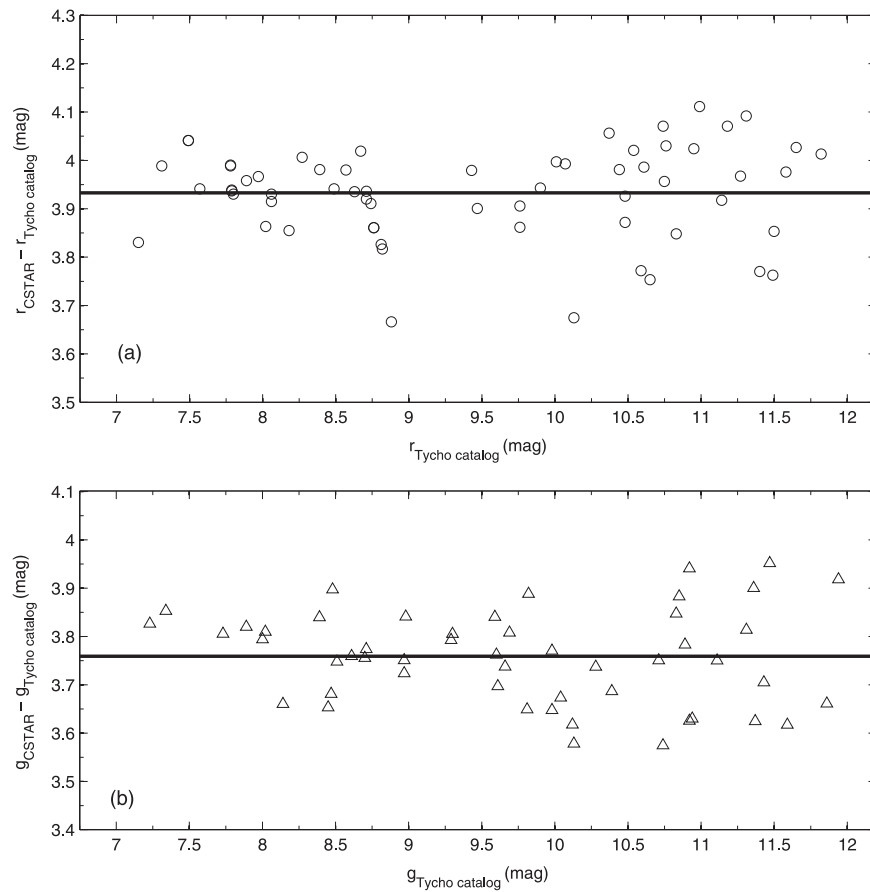
[15] http://vizier.u-strasbg.fr

**Figure 1.** Photometric calibration of CSTAR observations in the (a) *r* and (b) *g* bands.
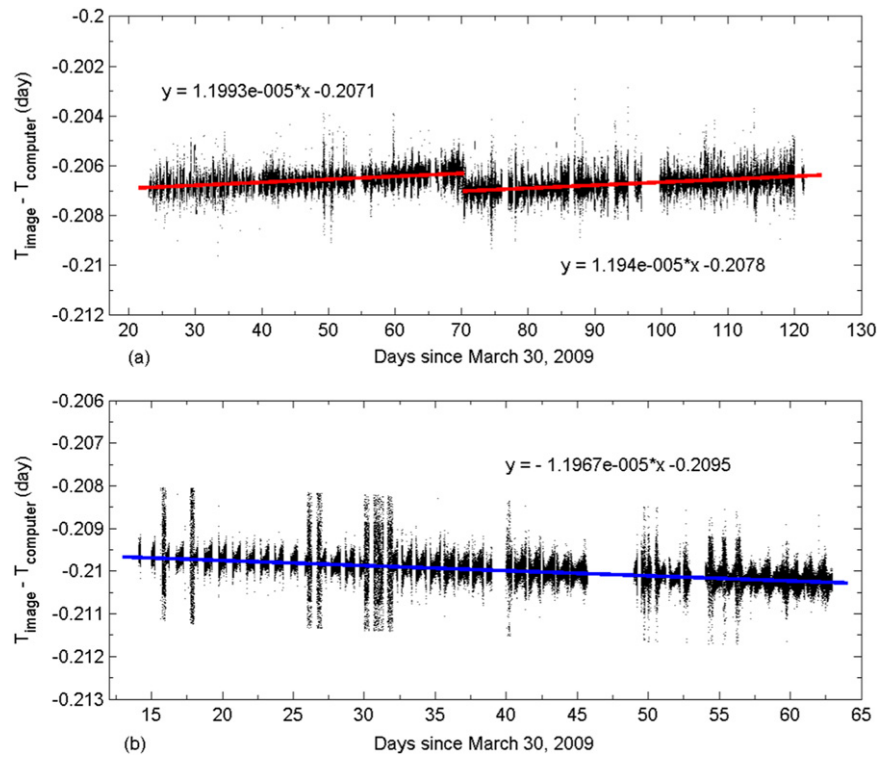


**Figure 2.** Difference between computer time and UTC in the (a) *r* and (b) *g* bands over the period of observation. The spikes in time residuals are caused by bad weather or high sky brightness. UTC was obtained from the star positions on the images, and the start time offsets were deduced by using the method described in Section 3.2.2. Linear fits are plotted as solid lines.
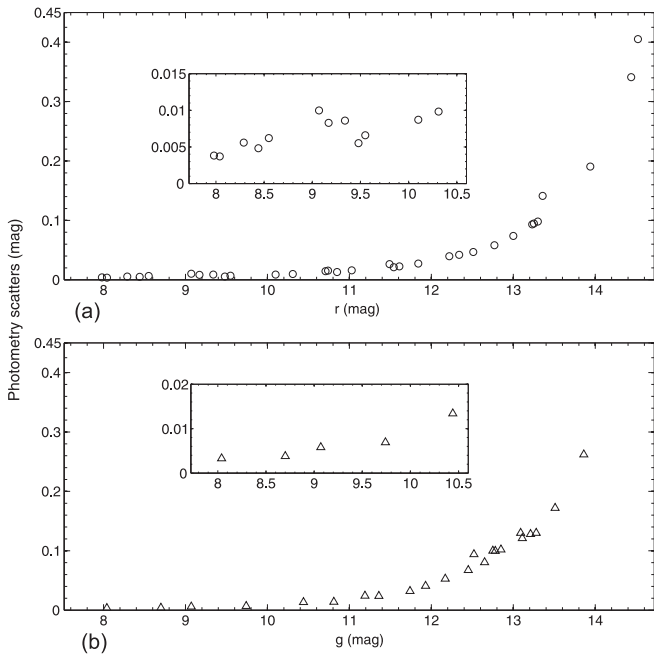
**Figure 3.** Photometric scatter diagram in the (a) $r$ and (b) $g$ bands for the images with an exposure time of 20 s. Circles show scatter in the $r$ band and triangles show scatter in the $g$ band. The inset zooms are for stars with an apparent magnitude in the range $7.8 < r, g < 10.6$. Note that the photometric precision for our target HD 92277 ($V = 9.^{m}10$) is about 7 and 9 mmag ($1\sigma$) in the $r$ and the $g$ band, respectively.

studying pulsating variables such as high-amplitude $\delta$ Scuti stars, Cepheids, and RR Lyrae stars. Stars with magnitudes $[r, g] > 13$ were observed with less precision, but, in principle, longer-term pulsations for such stars can be determined by averaging over many short exposures.

### 3.3.2. HD 92277

The photometric scatter is typically 6 mmag in the best observation conditions for our target HD 92277 in the $r$ band and near 8 mmag in the $g$ band. Note that the comparison star HD 93426 is nearly one mag fainter than the target HD 92277 in the $g$ band while their magnitudes are very similar in the $r$ band.

Figures 4 and 5 show the reduced light curves of HD 92277 in the $r$ and $g$ bands, respectively. The light curves of the second check star HD 99685 relative to the comparison star are derived in the $r$ and $g$ bands shown in Figures 6(a) and (b). Figure 7 shows the light curves of HD 99685 relative to the first check star HD 98784 in the $r$ and $g$ bands.

## 4. PULSATION ANALYSIS

We performed frequency analyses on the reduced light curves by using the software PERIOD04 (Lenz & Breger 2005). The software makes a search for significant peaks by calculating the amplitude spectra of the Fourier transform and fits the observed light curves with the following formula:

$$m = m_0 + \sum_i A_i \sin\left(2\pi\left(f_i t + \phi_i\right)\right).$$

The top panel of Figure 8(a) shows the Fourier amplitudes of the light curves in the $r$ band. We have resolved 89 peaks with a signal-to-noise ratio (S/N) above 4.0 (Breger et al. 1993;

Kuschnig et al. 1997) in the $r$ band for star HD 92277. Figure 4 shows the fitting curves with the 36 frequency solution in the $r$ band listed in Table 4. The unlisted 53 peaks (spurious frequencies; see Section 5.1 for details) have very tiny differences in fitting the light curves for HD 92277, same for the $g$-band light curves' fitting. Figure 9 shows the Fourier amplitudes from the frequency pre-whitening process for the $r$ band data.

The Fourier amplitudes of the data collected with the $g$-band telescope of CSTAR are shown in Figure 8(b), which presents a relatively larger noise level than the $r$-band data. We have detected 104 peaks with S/N above 4.0 in the $g$ band for star HD 92277. Figure 5 shows the fitting curves with the 27 frequency solution in the $g$ band listed in Table 4.

Since obvious variations with a period of one day are seen in Figures 6 and 7, we also performed frequency analyses on these light curves. We select the frequencies of two check stars' light curves as a reference to the frequencies detected from the data of the star HD 92277. The bottom panels of Figures 8(a) and (b) show the amplitude spectra of the check stars in the $r$ and $g$ bands, respectively.

## 5. DISCUSSION

### 5.1. The Pulsations

We have detected 89 frequencies in the $r$ band and 104 frequencies in the $g$ band with an S/N higher than 4.0. The frequencies are of two kinds: stellar pulsations and spurious frequencies that are not intrinsic to the star. The latter are included when fitting the light curves, but are not considered to be stellar oscillations of HD 92277. We list the stellar pulsation frequencies and the first 10 and 11 spurious frequencies in the $r$ and $g$ bands, respectively, in Table 4.

The detected stellar pulsations number 21 in the $r$ band and 14 in the $g$ band for the star HD 92277. The detected 20 and 13 frequencies are independent in the $r$ and $g$ bands, respectively. The primary frequency $f_1 = 10.810$ cd$^{-1}$ and the other 13 frequencies are detected in both bands, including one combination term $f_{12} = 18.123$ cd$^{-1}$. The primary frequency $f_1 = 10.810$ cd$^{-1}$ of HD 92277, the spectral type F0IV/V, and the 20 further independent frequencies lead us to categorize it as a new member of the $\delta$ Scuti star class with multi-period pulsations.

The spurious frequencies present in the Fourier transforms are believed to be caused by the observations running over a long period of time and by motions of each star as the sky rotates with respect to the telescope (which was fixed, not tracking) caused by imperfect optics. Four kinds of spurious frequencies are classified as follows: (1) the sidereal frequency $\nu_s = 1.0027$ cd$^{-1}$, mainly affected by the defects of the mirrors of the CSTAR telescopes and variations of sky brightness with the solar elevation; (2) the lunar frequency $\nu_l = 0.036$ cd$^{-1}$, mainly caused by the variations of sky brightness with the lunar elevation and phases; (3) the data frequency $\nu_d = 0.011$ cd$^{-1}$ in the $r$ band and $\nu_d = 0.023$ cd$^{-1}$ in the $g$ band, mainly a result of the length of the data sets; and (4) frequencies in the low-frequency domain ($<1.5$ cd$^{-1}$), induced mainly by variations in the atmospheric transparency and in the sensitivity of the CCD detectors. The frequencies from $f_{22}$ to $f_{26}$ are combinations of one independent pulsation frequency with one spurious frequency, two of which, $f_{22} = 9.252$ cd$^{-1}$ and $f_{25} = 24.856$ cd$^{-1}$, are detected in both bands.
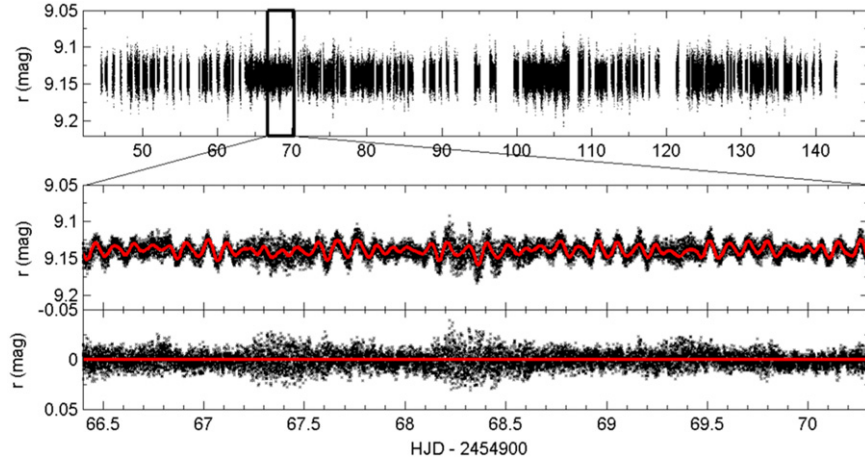
**Figure 4.** Light curves of HD 92277 in the *r* band in 2009 are plotted as dots. A part of the approximately 100 day time series in the top panel is expanded to a section covering about four days in time for the bottom panels. The solid curves in the middle panel show the result of fitting the 36 frequencies in the *r* band listed in Table 4. The residuals of fit are plotted in the bottom panel as dots, and the straight line shows the average value of the residuals. The data used to create this figure are available.
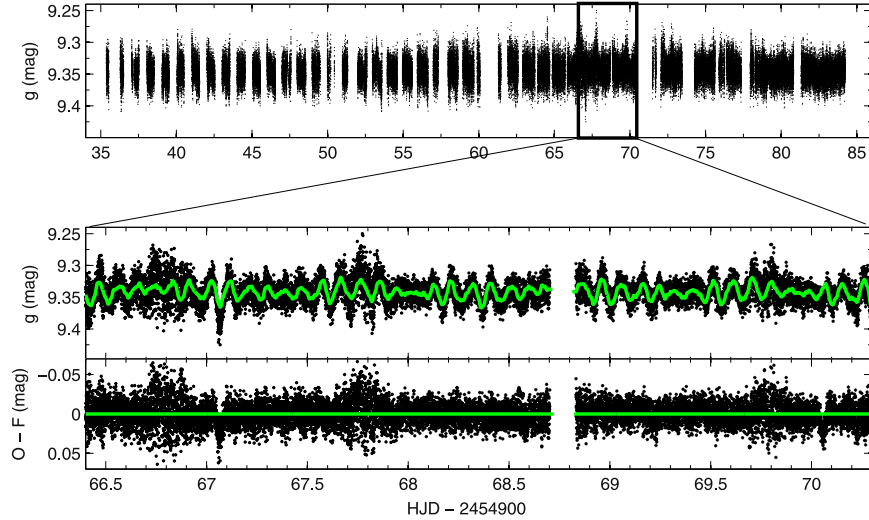


**Figure 5.** Light curves of HD 92277 in the *g* band in 2009 are plotted as dots. A part of the approximately 50 day time series in the top panel is expanded to a section covering about four days in time for the bottom panels. The solid curves in the middle panel show the result of fitting the 27 frequencies in the *g* band listed in Table 4. The residuals of fit are plotted in the bottom panel as dots and the straight line shows the average value of the residuals. The data used to create this figure are available.

### 5.2. Steps Toward Mode Identification

The oscillation amplitude of HD 92277 is 0.03 mag and 0.04 mag in the *r* and *g* bands, respectively. The color index $g - r = 0.2$ was calculated from the data sets, and we used the equation (Jester et al. 2005):

$$B - V = 0.90 \times (g - r) + 0.21$$

to derive $B - V = 0.39 \pm 0.03$, which is in good agreement with the value $B - V = 0.375$ reported by van Leeuwen (2007). Using the parallax $2.12 \pm 0.91$ mas and $V = 9.10$ values mentioned in Section 1, we derived an absolute magnitude $M_V = 0.73\pm^{0.78}_{1.22}$ in the *V* band. The effective temperature $T_{\rm eff} = 6800\pm^{170}_{150}$ K can be estimated based on $B - V = 0.39 \pm 0.03$ and the empirical formula (Swamy 1996)

$$T_{\rm eff} = 8540/[(B - V) + 0.865],$$

where we adopted the bolometric correction BC = 0.022 from Table 3 of Flower (1996), obtaining $M_{\rm bol} = 0.75\pm^{0.78}_{1.22}$.

The empirical mass–luminosity relation for a star of $M \geqslant 0.43\,M_\odot$ is approximately $\log (L/L_\odot) = 4 \log (M/M_\odot)$. Using the relation of $M_{\rm bol} - M_{\rm bol,\odot} = 2.5 \log (L_\odot/L)$ and adopting the following solar values taken from Sun Fact Sheet[16]: $T_{\rm eff,\odot} = 5778$ K, $\log g_\odot = 4.4378$, and $M_{\rm bol,\odot} = 4.83$, one obtains

$$\log g = 0.3 M_{\rm bol} + 4 \log T_{\rm eff} - 12.035. \tag{1}$$

The pulsation constant, *Q*, of a δ Scuti star is defined by the period–density relation:

$$P\sqrt{\frac{\rho}{\rho_\odot}} = Q,$$

which can be rearranged in the form,

$$\log Q = -6.454 + \log P + 0.5 \log g + 0.1 M_{\rm bol} + \log T_{\rm eff}. \tag{2}$$
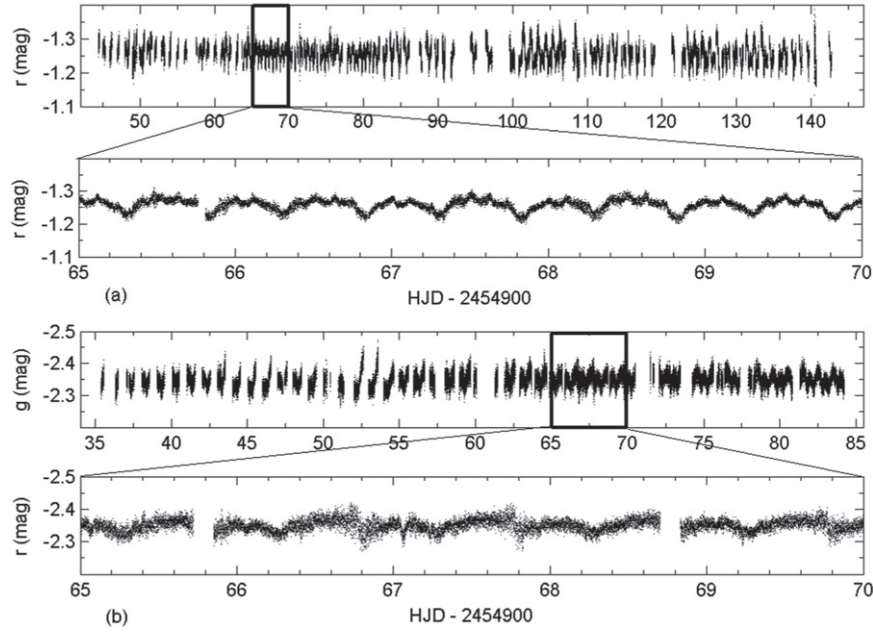
---

[16] http://nssdc.gsfc.nasa.gov

**Figure 6.** Light curves of the second check star HD 99685 relative to the comparison star HD 93426 in the (a) *r* and (b) *g* bands.
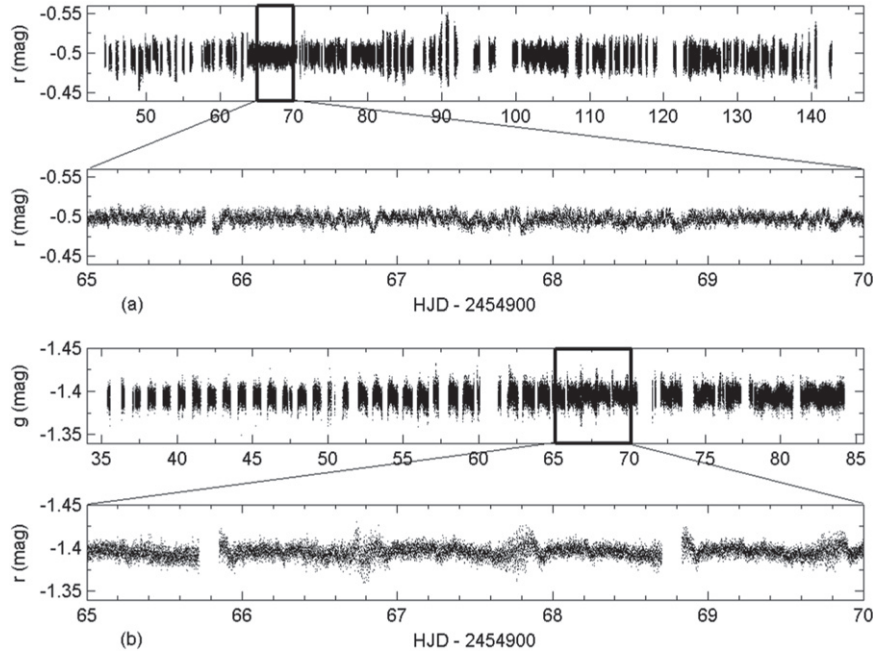


**Figure 7.** Light curves of the second check star HD 99685 relative to the first check star HD 98784 in the (a) *r* and (b) *g* bands.

From Equations (1) and (2), we obtain the pulsation constant

$$\log Q = \log P + 0.25 M_{\rm bol} + 3 \log T_{\rm eff} - 12.471.$$

Finally, using $T_{\rm eff} = 6800 \pm^{170}_{150}$ K and $M_{\rm bol} = 0.75 \pm^{0.78}_{1.22}$ in the above equation, we find $Q_1 = 0.015 \pm 0.007$ days and $Q_2 = 0.018 \pm 0.009$ days for the primary and secondary frequencies, respectively, indicating both the pulsations in the low overtone *p* modes. The lack of observational parameters such as $\log g$ hinders our ability to obtain more precise pulsation constants of these frequencies. Hence, it is impossible to make further mode identifications based on the *Q* values of these frequencies alone.

An alternative method of mode identification is the examination of amplitude ratios and phase variations of measurements at different wavelengths (Balona & Stobie 1980; Watson 1988; Garrido et al. 1990). The variations in two color bands observed at the same time during the 2009 observational duty of CSTAR telescopes were used to derive phase shift and amplitude ratio values for the first two frequencies. We first transformed *g* and *r* magnitudes into *B* and *V* magnitudes by using the following equation (Jester et al. 2005):

$$V = g - 0.58 \times (g - r) - 0.01.$$

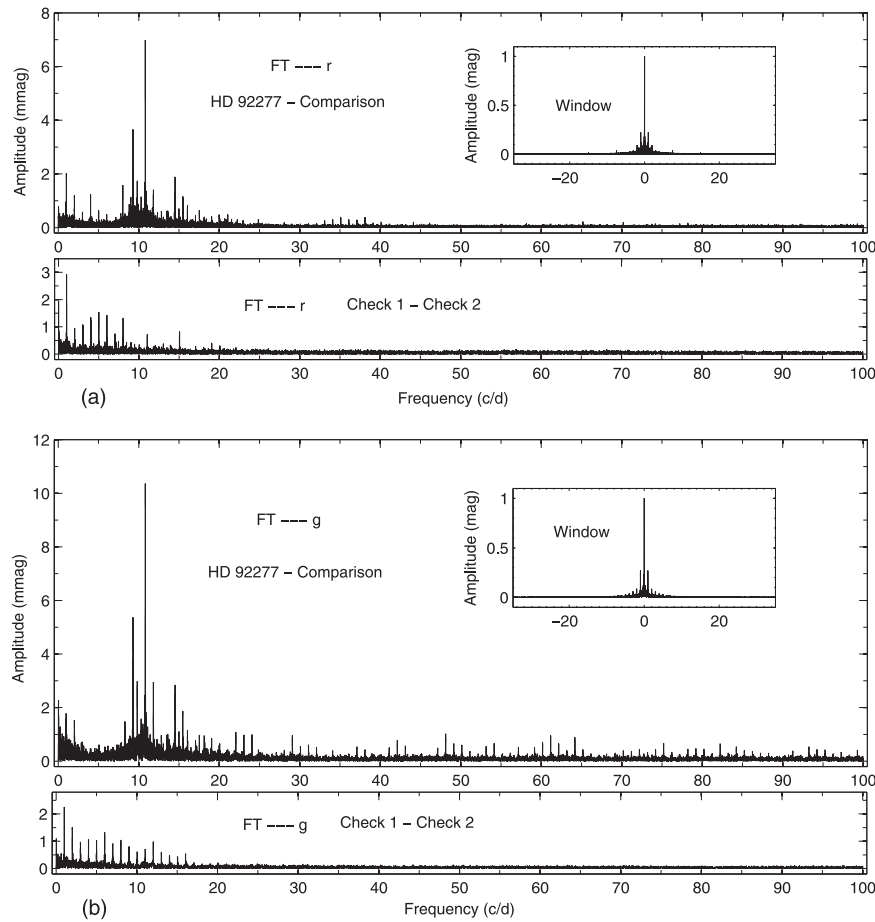Then, we made a series of Fourier transforms of the data sets in

**Figure 8.** Fourier amplitude spectra of CSTAR data in 2009 for HD 92277 in the (a) *r* and (b) *g* bands in the top panels. The corresponding window functions are shown in the inset panels. The bottom panels show the Fourier transforms of the light curves of the first check star relative to the second check star.

both bands observed at the same time, changing the start offset time in a range with the uncertainty of 0.0006 days. The amplitude ratios of frequency $f_1$ and $f_2$ are $A_{B-V}/A_V = 0.360 \pm 0.004$ and $0.407 \pm 0.005$, respectively. The phase shift of frequency $f_1$ is $\phi_{B-V} - \phi_V = -5.7 \pm 4°6$. The position of mode $f_1$ is shown in Figure 10, which suggests that frequency $f_1$ is more likely to be an $l = 1$ mode (Watson 1988). However, the value of the phase shift of frequency $f_2$ has a very large uncertainty that prohibits any further attempt at mode identification. The upgraded CTSAR telescopes, with the tracking mount and a working GPS time source, will greatly reduce the number of spurious frequencies and would identify more oscillation modes of HD 92277 based on their values of the amplitude ratio and the phase shift.

### 5.3. Limitations of CSTAR

The discovery of the new $\delta$ Scuti star HD 92277, with more than a dozen independent frequencies of oscillation, shows some potential of conducting continuous multi-color photometry from Dome A, Antarctica. Apart from the frequencies intrinsic to the star, dozens of spurious frequencies were seen in the light curves of HD 92277—these are believed to be inevitable when using small aperture telescopes with a wide FOV, without tracking, and over a long period of time (so, e.g., changes in the sky background with the phase of the Moon have an effect). We should be able to reduce the amplitude of

the spurious frequencies by using an ensemble of reference stars close in decl. to HD 92277 so that they trace the same circles on the CCD frame over a sidereal day. Such methods had been employed with data from the *i*-band telescope (Meng et al. 2013) in order to increase the photometric precision of the CSTAR catalog, but this is beyond the scope of the present paper.

Space missions can, of course, obtain much higher-precision photometry than any ground-based telescope, although usually unfiltered or monochrome. For example, the very precise photometry from the *CoRoT* mission makes it possible to study several $\delta$ Scuti stars at the noise level of a few 100th of mmag, resolving several hundreds of frequencies in $\delta$ Scuti stars such as HD 50844 (Poretti et al. 2009) and HD 174836 (García Hernández et al. 2009), and to discover modulation effects such as those found in the light curve of the high-amplitude $\delta$ Scuti star *CoRoT* 101155310 (Poretti et al. 2011). The *Kepler* space mission continuously monitored hundreds of $\delta$ Scuti stars with >90% duty circles for four years up to 2013 May with $\mu$mag precision. These data are of unprecedented quality and give several striking results such as the regularity seen in the frequencies of the $\delta$ Scuti star KIC 8054146 (Breger et al. 2012), the discovery of solar-like oscillations in the $\delta$ Scuti star HD 187547 (Antoci et al. 2011), and $\sim$23% $\delta$ Scu/$\gamma$ Dor hybrids in pulsating A–F type stars (Uytterhoeven et al. 2011).

**Table 4**
Multi-frequency Solution of the Light Curves of HD 92277 in the $r$ and $g$ Bands from CSTAR in 2009

| ID | Type | Frequency $(\mathrm{cd}^{-1})$ | $r$-band Amplitude (mmag) | S/N | Frequency $(\mathrm{cd}^{-1})$ | $g$-band Amplitude (mmag) | S/N | Note |
|---|---|---|---|---|---|---|---|---|
| $f_1$ | $\cdots$ | 10.810 | 6.86 | 99.0 | 10.810 | 10.34 | 66.1 | $\cdots$ |
| $f_2$ | $\cdots$ | 9.285 | 3.24 | 46.2 | 9.285 | 5.00 | 34.7 | $\cdots$ |
| $f_3$ | $\cdots$ | 14.505 | 1.77 | 29.3 | 14.505 | 2.87 | 20.5 | $\cdots$ |
| $f_4$ | $\cdots$ | 9.336 | 1.26 | 17.9 | 9.335 | 1.63 | 11.1 | $\cdots$ |
| $f_5$ | $\cdots$ | 15.468 | 1.22 | 19.4 | 15.469 | 1.86 | 14.9 | $\cdots$ |
| $f_6$ | $\cdots$ | 13.608 | 0.72 | 11.4 | 13.609 | 0.90 | 6.3 | $\cdots$ |
| $f_7$ | $\cdots$ | 14.990 | 0.70 | 11.5 | 14.992 | 0.98 | 7.5 | $\cdots$ |
| $f_8$ | $\cdots$ | 17.522 | 0.60 | 9.4 | 17.522 | 0.99 | 6.5 | $\cdots$ |
| $f_9$ | $\cdots$ | 9.505 | 0.58 | 8.2 | 9.502 | 0.62 | 4.2 | $\cdots$ |
| $f_{10}$ | $\cdots$ | 19.980 | 0.50 | 7.9 | 19.982 | 0.83 | 6.7 | $\cdots$ |
| $f_{11}$ | $\cdots$ | 7.313 | 0.49 | 8.4 | 7.313 | 0.75 | 5.4 | $\cdots$ |
| $f_{12}$ | $f_1 + f_{11}$ | 18.123 | 0.45 | 6.9 | 18.124 | 0.90 | 6.1 | $\cdots$ |
| $f_{13}$ | $\cdots$ | 13.666 | 0.41 | 6.5 | 13.665 | 0.74 | 5.1 | $\cdots$ |
| $f_{14}$ | $\cdots$ | 7.835 | 0.37 | 6.0 | $\cdots$ | $\cdots$ | $\cdots$ | $\cdots$ |
| $f_{15}$ | $\cdots$ | 13.646 | 0.36 | 5.7 | $\cdots$ | $\cdots$ | $\cdots$ | $\cdots$ |
| $f_{16}$ | $\cdots$ | 17.770 | 0.33 | 5.1 | $\cdots$ | $\cdots$ | $\cdots$ | $\cdots$ |
| $f_{17}$ | $\cdots$ | 15.143 | 0.32 | 5.0 | 15.143 | 0.65 | 4.9 | $\cdots$ |
| $f_{18}$ | $\cdots$ | 15.245 | 0.28 | 4.6 | $\cdots$ | $\cdots$ | $\cdots$ | $\cdots$ |
| $f_{19}$ | $\cdots$ | 8.545 | 0.27 | 4.1 | $\cdots$ | $\cdots$ | $\cdots$ | $\cdots$ |
| $f_{20}$ | $\cdots$ | 10.779 | 0.26 | 4.0 | $\cdots$ | $\cdots$ | $\cdots$ | $\cdots$ |
| $f_{21}$ | $\cdots$ | 22.242 | 0.23 | 4.4 | $\cdots$ | $\cdots$ | $\cdots$ | $\cdots$ |
| $f_{22}$ | $f_2 - \nu_l$ | 9.253 | 1.78 | 25.5 | 9.252 | 2.69 | 19.0 | lunar |
| $f_{23}$ | $f_3 + 7\nu_s$ | 21.527 | 0.28 | 4.8 | $\cdots$ | $\cdots$ | $\cdots$ | sidereal |
| $f_{24}$ | $f_1 + 10\nu_s$ | 20.847 | 0.35 | 5.7 | $\cdots$ | $\cdots$ | $\cdots$ | sidereal |
| $f_{25}$ | $f_1 + 14\nu_s$ | 24.856 | 0.30 | 5.6 | 24.856 | 0.54 | 4.7 | sidereal |
| $f_{26}$ | $f_{19} + 4\nu_s$ | 12.545 | 0.29 | 4.5 | $\cdots$ | $\cdots$ | $\cdots$ | sidereal |
| $F_1$ | $\nu_s$ | 1.004 | 2.34 | 27.9 | 1.006 | 2.57 | 18.7 | sidereal |
| $F_2$ | $8\nu_s$ | 8.021 | 1.56 | 24.4 | $\cdots$ | $\cdots$ | $\cdots$ | sidereal |
| $F_3$ | $4\nu_s$ | 4.011 | 1.29 | 16.3 | 4.001 | 1.16 | 8.1 | sidereal |
| $F_4$ | $2\nu_s$ | 2.005 | 1.12 | 13.3 | 2.002 | 2.03 | 14.6 | sidereal |
| $F_5$ | $9\nu_s$ | 9.020 | 0.79 | 11.5 | 9.008 | 0.85 | 6.1 | sidereal |
| $F_6$ | $\nu_d$ | 0.011 | 0.94 | 12.1 | 0.023 | 3.87 | 32.0 | data |
| $F_7$ | $\cdots$ | 0.965 | 0.70 | 8.6 | 0.966 | 0.68 | 4.9 | ? |
| $F_8$ | $\cdots$ | 0.572 | 0.61 | 7.8 | $\cdots$ | $\cdots$ | $\cdots$ | ? |
| $F_9$ | $\cdots$ | 0.144 | 0.61 | 7.7 | 0.141 | 1.06 | 8.5 | ? |
| $F_{10}$ | $\nu_l(2\nu_l)$ | 0.034 | 0.41 | 5.2 | 0.067 | 1.45 | 11.9 | lunar |
| $F_{11}$ | $\cdots$ | $\cdots$ | $\cdots$ | $\cdots$ | 0.223 | 1.74 | 4.9 | ? |
| $F_{12}$ | $\cdots$ | $\cdots$ | $\cdots$ | $\cdots$ | 0.419 | 1.54 | 14.6 | ? |
| $F_{13}$ | $48\nu_s$ | $\cdots$ | $\cdots$ | $\cdots$ | 48.126 | 1.08 | 10.6 | sidereal |

**Notes.** $\nu_s = 1.0027$ $\mathrm{cd}^{-1}$, $\nu_l = 0.036$ $\mathrm{cd}^{-1}$, $\nu_d = 0.011$ $\mathrm{cd}^{-1}$ in the $r$ band and $\nu_d = 0.029$ $\mathrm{cd}^{-1}$ in the $g$ band. The "sidereal" flag means that the frequency is likely influenced by the Earth rotation, the "lunar" flag means that the frequency may be related to the moon phase, the "?" flag means that the frequency is in the low-frequency domain ($<1.5$ c/d), and the "data" flag means that the frequency is likely influenced by the length of the data set. The spurious frequencies have subscripts $s$, $l$, and $d$, corresponding to the origin in the source indicated by the flags noted above (see the rightmost column).

## 6. SUMMARIES, CONCLUSIONS, AND PROSPECTS

We have reported high-quality time-series photometry for HD 92277 in two bands, $g$ and $r$, from the CSTAR telescopes during the winter of 2009 from Dome A, Antarctica. The total exposure times were 694 and 1264 hr in the $g$ and $r$ bands, respectively. We detected 21 frequencies in the $r$ band and 14 frequencies in the $g$ band, 14 of which were detected in both bands. The primary frequency $f_1$ is more likely an $l = 1$ $p$-mode, based on the amplitude ratios and phase variations of the modes. HD 92277 is classified as a new $\delta$ Scuti star based on its spectral type and the primary frequency corresponding to a period of 0.0925 days. The pulsation constant values $Q$ for the first two frequencies were estimated by using empirical formulae.

HD 92277 is the first asteroseismic target observed from Dome A and shows multi-period oscillations. Our work shows that multi-color observations bring valuable information to help with the mode identification of the pulsations and show how ground-based multi-color asteroseismology has some advantages over monochrome data from space missions. Unfortunately, since very few observations have been made of HD 92277 before, the star lacks precise physical parameters such as $\log g$, metallicity $[M/H]$, and projected rotational velocity $v \sin i$. Spectroscopic observations are particularly needed for further investigations, such as testing the detected frequencies by using seismic models and determining the evolutionary status and mass of HD 92277 by using stellar evolution models such as the MESA code (Paxton et al. 2011).
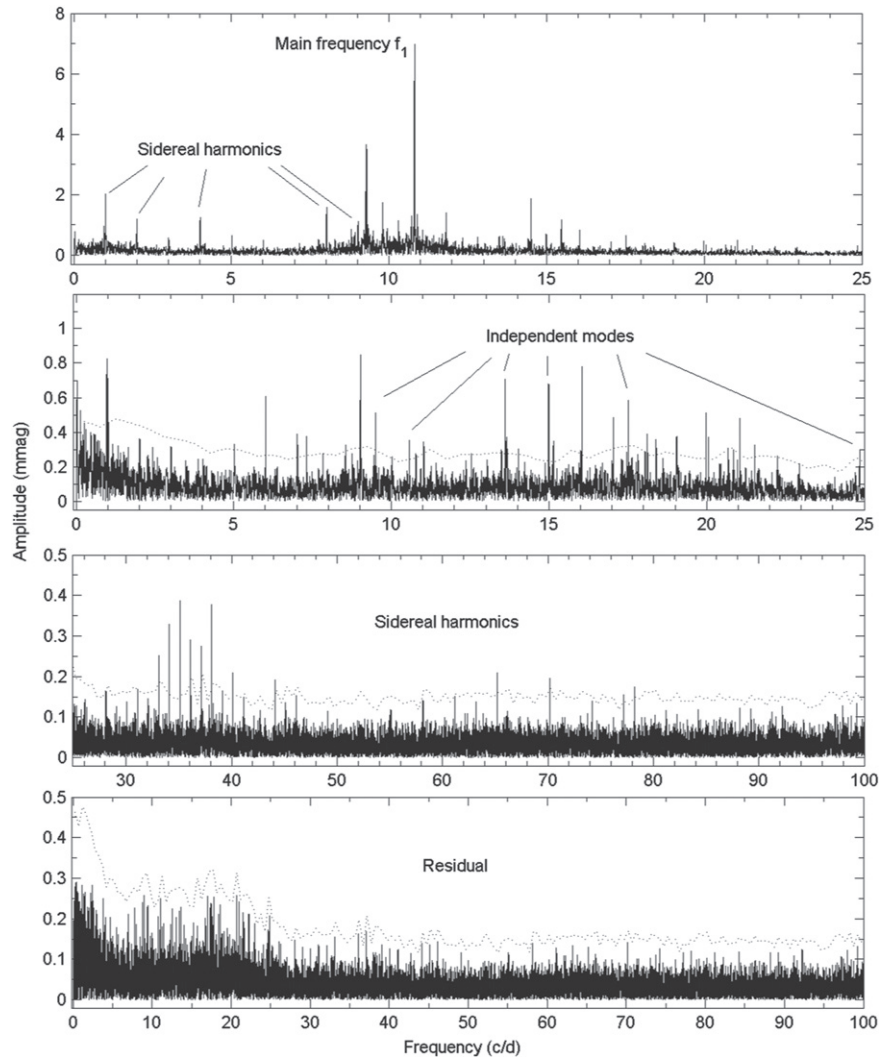
**Figure 9.** Subsequent steps of the extraction of frequencies in the amplitude spectra of HD 92277 in the $r$ band. The dashed lines in the panels indicate the $4\sigma$ confidence levels. Note that the scales of the coordinates of the four panels may be different from each other.

CSTAR, the prototype instrument for photometry deployed at Dome A, has been operated since 2008 for four winters and will be re-deployed in 2015 January with improvements, including a tracking mount and a working GPS time source. The upgraded CTSAR telescopes will greatly reduce the number of spurious frequencies and will identify more oscillation modes in pulsating stars, including HD 92277, based on their values of the amplitude ratio and the phase shift. The scientific results from CSTAR, together with those from other instruments deployed at Dome A, show that the observational conditions are better in many respects than temperate sites. Dome A offers well in excess of 1000 hr of photometric time with a $>60\%$ duty cycle every year, with low scintillation noise, long periods (weeks) of continuously good conditions, no diurnal aliasing in winter, and low air mass variations as a result of the extreme southern latitude. These factors all make precision photometry possible and are especially important for asteroseismology. The 14.5 cm CSTAR telescopes can effectively monitor bright targets around the south celestial pole. The weather is the fundamental limitation for CSTAR, as it is for all ground-based telescopes. Other limitations include low-frequency drifts in CCD sensitivity and small focus changes.
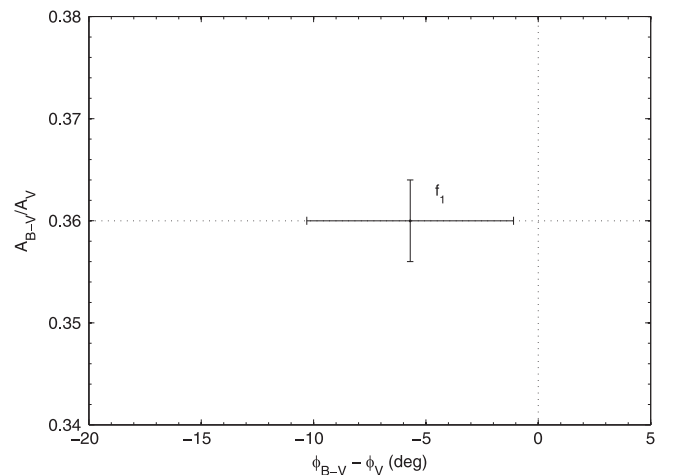


**Figure 10.** Phase shift and amplitude ratio of the primary frequency $f_1$ determined from CSTAR photometry in the $r$ and $g$ bands.

The first of three AST3 telescopes, the successor of CSTAR, was installed at Dome A in 2012 January and a second AST3 is planned to be installed there in 2015 January. The AST3

telescopes will monitor parts of the southern sky in one month time blocks and will offer high-quality photometric data in three different bands, *G*, *R* and *I*, to provide important information for mode identification for pulsating stars, which monochrome space missions such as *CoRoT* and *Kepler* cannot do. Obviously, pulsators in the FOV of AST3 will spread over the entire H-R diagram since the targets can be as faint as $I = 19.5$ mag. KDUST, the third-generation Chinese Antarctic telescope, with a 2.5 m aperture is now being designed (Yuan et al. 2013) and could make follow-up observations of interesting pulsating targets. Time-series spectroscopic observations conducted by KDUST would be very valuable for asteroseismology. By comparing the spectroscopic and photometric observations with stellar models, it would assist with a precise determination of oscillation modes from which one could learn more details of the internal structure of the stars.

## REFERENCES

Antoci, V., Handler, G., Campante, T. L., et al. 2011, Natur, 477, 570
Ashley, M. C. B. 2013, in IAU Symp. 288, Astrophysics in Antarctica, ed. T. Montmerle et al. (Cambridge: Cambridge Univ. Press), 15
Baglin, A., Auvergne, M., Boisnard, L., et al. 2006, in 36th COSPAR Scientific Assembly, ed. M. A. Shea (Amsterdam: Elsevier), 3749
Balona, L. A., & Stobie, R. S. 1980, MNRAS, 190, 931
Bonner, C. S., Ashley, M. C. B., Lawrence, J. S., Luong-Van, D. M., & Storey, J. W. V. 2010, PASP, 122, 1122
Borucki, W. J., Koch, D., Basri, G., et al. 2010, Sci, 327, 977
Breger, M. 2000, in ASP Conf. Ser. 210, Delta Scuti and Related Stars, ed. M. Breger, & M. Montgomery (San Francisco, CA: ASP), 3
Breger, M., Fossati, L., Balona, L., et al. 2012, A&A, 759, 62
Breger, M., Stich, J., Garrido, R., et al. 1993, A&A, 271, 482
Deeg, H. J., Belmonte, J. A., Alonso, R., et al. 2005, in EAS Publ. Ser. 14, Dome C Astronomy and Astrophysics Meeting, ed. M. Giard et al. (Les Ulis: EDP Sciences), 303
Fabricius, C., & Makarov, V. V. 2000, A&A, 356, 141
Flower, P. J. 1996, ApJ, 469, 355
Fossat, E. 2005, in EAS Publ. Ser. 14, Dome C Astronomy, and Astrophysics Meeting, ed. M. Giard et al. (Les Ulis: EDP Sciences), 121
García Hernández, A., Moya, A., Michel, E., et al. 2009, A&A, 506, 79
Garrido, R., Garcia-Lobo, E., & Rodriguez, E. 1990, A&A, 234, 262
Harvey, J. W., Hill, F., Hubbard, R., et al. 1996, Sci, 272, 1284
Høg, E., Fabricius, C., Makarov, V. V., et al. 2000, A&A, 355, L27
Houck, N., & Cowley, A. P. 1975, University of Michigan, Catalogue of two-dimensional spectral types for the HD stars (Strasbourg: Stellar Data Center)
Jester, S., Schneider, D. P., Richards, G. T., et al. 2005, AJ, 130, 873
Kaye, A. B., Handler, G., Krisciunas, K., et al. 1999, PASP, 111, 840
Kuschnig, R., Weiss, W. W., Gruber, R., et al. 1997, A&A, 328, 544
Lawrence, J. S., Ashley, M. C. B., Tokovinin, A., & Travouillon, T. 2004, Natur, 431, 378
Lawrence, J. S., Ashley, M. C. B., Hengst, S., et al. 2009, RScT, 80, 064501
Lenz, P., & Breger, M. 2005, CoAst, 146, 53
Liu, G., & Yuan, X. 2009, AcASn, 50, 224
Matthews, J. M. 2007, CoAst, 150, 333
Meng, Z., Zhou, X., Zhang, H., et al. 2013, PASP, 125, 1015
Michel, E., Belmonte, J. A., Alvarez, M., et al. 1992, A&A, 255, 139
Mosser, B., & Aristidi, E. 2007, PASP, 119, 127
Nather, R. E., Winget, D. E., Clemens, J. C., Hansen, C. J., & Hine, B. P. 1990, ApJ, 361, 309
Ofek, E. O. 2008, PASP, 120, 1128
Okita, H., Ichikawa, T., Ashley, M. C. B., Takato, N., & Motoyama, H. 2013, A&A, 554, L5
Paxton, B., Bildsten, L., Dotter, A., et al. 2011, ApJS, 192, 3
Pont, F., & Bouchy, F. 2005, in EAS Publ. Ser., 14, Dome C Astronomy and Astrophysics Meeting, ed. M. Giard et al. (Les Ulis: EDP Sciences), 155
Poretti, E., Michel, E., Garrido, R., et al. 2009, A&A, 506, 85
Poretti, E., Rainer, M., Weiss, W. W., et al. 2011, A&A, 528, 147
Stankov, A., & Handler, G. 2005, ApJS, 158, 193
Saunders, W., Lawrence, J. S., Storey, J. W. V., et al. 2009, PASP, 121, 976
Sims, G., Ashley, M. C. B., Cui, X., et al. 2012, PASP, 124, 637
Strassmeier, K. G., & Oláh, K. 2004, in Second Eddington Workshop: Stellar Structure and Habitable Planet Finding, ed. F. Favata, S. Aigrain, & A. Wilson (ESA SP-538; Noordwijk: ESA), 149
Strassmeier, K. G., Briguglio, R., Granzer, T., et al. 2008, A&A, 490, 287
Swamy, S. 1996, Astrophysics: A Modern Prospective (New Delhi: New Age International Publishers)
Uytterhoeven, K., Moya, A., Grigahcène, A., et al. 2011, A&A, 534, A135
van Leeuwen, F. 2007, A&A, 474, 653
Wang, L., Macri, L. M., Krisciunas, K., et al. 2011, AJ, 142, 155
Wang, L., Macri, L. M., Wang, L., et al. 2013, AJ, 146, 139
Watson, R. D. 1988, Ap&SS, 140, 255
Yang, H., Allen, G., Ashley, M. C. B., et al. 2009, PASP, 121, 174
Yuan, X., Cui, X., Gong, X., et al. 2010, Proc. SPIE 7733, 77331V
Yuan, X., Cui, X., Su, D., et al. 2013, in IAU Symp. 288, Astrophysics from Antarctica, ed. T. Montmerle et al. (Cambridge: Cambridge Univ. Press), 271
Zhou, X., Fan, Z., Jiang, Z., et al. 2010, PASP, 122, 347
Zhou, X., Wu, Z., Jiang, Z., et al. 2010, RAA, 10, 279
Zong, W., Fu, J., Niu, J., et al. 2014, AR&T, 11, 89
Zou, H., Zhou, X., Jiang, Z., et al. 2010, AJ, 140, 602